

# Low-Dimensional Long-Range Topological Charge Structure in the QCD Vacuum

I. Horváth<sup>a</sup>, S.J. Dong<sup>a</sup>, T. Draper<sup>a</sup>, F.X. Lee<sup>b,c</sup>, K.F. Liu<sup>a</sup>, N. Mathur<sup>a</sup>, H.B. Thacker<sup>d</sup> and J.B. Zhang<sup>e</sup>

<sup>a</sup>Department of Physics, University of Kentucky, Lexington, KY 40506

<sup>b</sup>Center for Nuclear Studies and Department of Physics, George Washington University, Washington, DC 20052

<sup>c</sup>Jefferson Lab, 12000 Jefferson Avenue, Newport News, VA 23606

<sup>d</sup>Department of Physics, University of Virginia, Charlottesville, VA 22901

<sup>e</sup>CSSM and Department of Physics, University of Adelaide, Adelaide, SA 5005, Australia

(Dated: September 15, 2003)

While sign-coherent 4-dimensional structures cannot dominate topological charge fluctuations in the QCD vacuum at all scales due to reflection positivity, it is possible that enhanced coherence exists over extended space-time regions of lower dimension. Using the overlap Dirac operator to calculate topological charge density, we present evidence for such structure in pure-gluon SU(3) lattice gauge theory. It is found that a typical equilibrium configuration is dominated by two oppositely-charged sign-coherent *connected* structures (“*sheets*”) covering about 80% of space-time. Each sheet is built from elementary 3-d cubes connected through 2-d faces, and approximates a low-dimensional curved manifold (or possibly a fractal structure) embedded in the 4-d space. At the heart of the sheet is a “*skeleton*” formed by about 18% of the most intense space-time points organized into a global *long-range* structure, involving connected parts spreading over maximal possible distances. We find that the skeleton is locally 1-dimensional and propose that its geometrical properties might be relevant for understanding the possible role of topological charge fluctuations in the physics of chiral symmetry breaking.

PACS numbers: 11.15.Ha, 11.30.Rd

One of the important goals in hadronic physics is a detailed understanding of vacuum structure in QCD. Local patterns in topological charge fluctuations represent an important aspect of this structure. Indeed, phenomena such as large  $\eta'$  mass,  $\theta$ -dependence, and possibly spontaneous chiral symmetry breaking (S $\chi$ SB) are directly related to vacuum fluctuations of topological charge. While lattice gauge theory provides a framework for first-principles non-perturbative studies of topological charge fluctuations, the extraction of meaningful and unbiased structural information has long been a difficult problem. However, the recent development of fermionic methods has improved this situation considerably and it is no longer necessary to rely on subjective procedures to smooth out the rough short-distance behavior of gauge fields. One way to proceed is to study the structure of low-lying Dirac eigenmodes and to infer the properties of underlying topological charge fluctuations indirectly. This was advocated in [1], developed in [2], and used in many recent studies (see e.g. [3, 4]).

The advances in implementing lattice chiral symmetry (for reviews see e.g. [5]) have also made it possible to pursue a *direct* approach to this problem. Indeed, with any  $\gamma_5$ -Hermitian lattice Dirac operator  $D$  satisfying the Ginsparg-Wilson relation  $\{D, \gamma_5\} = D\gamma_5 D$  (e.g. the overlap operator [6]), one can associate a topological charge density operator [7]

$$q_x = -\text{tr} \gamma_5 \left(1 - \frac{1}{2} D_{x,x}\right) \quad (1)$$

The global charge associated with this lattice density is strictly stable with respect to generic local variations of the gauge field [8], thus fully respecting the topological nature of this quantity. In addition, the above  $q_x$  is spe-

cial in several ways. For example, the index theorem is exactly satisfied with respect to the associated Dirac operator [7], and its renormalization properties are analogous to those in the continuum [9]. An important virtue of  $q_x$  is that it can be naturally eigenmode-expanded. While  $q_x$  contains all fluctuations up to the lattice cutoff, one can use the eigenmode expansion up to scale  $\Lambda$  to define an *effective density* [10],  $q_x^{(\Lambda)} \equiv -\sum_{|\lambda| \leq \Lambda} (1 - \frac{\lambda}{2}) c_x^\lambda$ , where  $c_x^\lambda = \psi_x^{\lambda\dagger} \gamma_5 \psi_x^\lambda$  is the local chirality of the mode with eigenvalue  $\lambda$ . The ultraviolet fluctuations are naturally filtered out in  $q_x^{(\Lambda)}$  (*eigenmode filtering* [2]), and this density can be used to study the structure of topological charge fluctuations at arbitrary low-energy scale  $\Lambda$ . By studying the effective densities, it was demonstrated [10] that topological charge at low energy is not locally concentrated in sign-coherent unit-quantized lumps (e.g. instantons). This was first predicted by Witten [11] and emphasized recently in [2], where the first lattice evidence was presented.

In this work, we initiate the investigation of possible non-trivial structure (order) in the *full* topological charge density Eq. (1) for typical configurations contributing to the pure gluon QCD path integral. This is a qualitatively new step with some aspects worth emphasizing. (a) We evaluate the local operator  $q_x$  at every space-time point, thus producing gauge invariant “configurations” of topological charge density. No processing of the underlying gauge configurations is involved and no bias is imposed. (b) Assuming that the well-defined space-time structure in  $q_x$  exists, it has to be viewed as *fundamental* (rather than low-energy) since, unlike the case of effective densities  $q_x^{(\Lambda)}$ , the use of a local operator does not introduce a new scale apart from the lattice cutoff already

in place. Consequently, such structure could have both short and long-distance manifestations. (c) A fundamental structure of this type has not been observed before in an unbiased setting. Indeed, using the conventional operators, the resulting space-time distributions of topological charge can hardly be distinguished from complete disorder. The common interpretation of this is that the physically relevant fluctuations might be obscured by the structureless ultraviolet noise arising due to entropy considerations (the problem of ultraviolet dominance).

In what follows, we will present evidence for the existence of fundamental structure in topological charge density, and demonstrate some of its basic geometric features. Needless to say, we do this with the aim that some of these properties might help to advance our understanding of the QCD vacuum, and hence of the basic features of hadronic physics. With regard to the problem of ultraviolet dominance, we were motivated by the fact that, apart from beautiful properties mentioned above, the operator  $q_x$  of Eq. (1) differs from standard lattice discretizations in a very qualitative manner. In particular, it is well-known that lattice chiral symmetry implies non-ultralocality of lattice Dirac kernel  $D$ , i.e. non-zero coupling among fermionic variables at arbitrarily large distances [12]. Similarly, it is believed that any  $D_{xy}$  involves gauge paths (from  $x$  to  $y$ ) running arbitrarily far from  $x$  and  $y$ . As a result,  $q_x$  will receive (small) contributions from arbitrarily extended gauge loops (*chiral smoothing* [2]) and is expected to be much less sensitive to the ultraviolet noise than typical ultralocal operators. We find that chiral smoothing indeed provides enough suppression of ultraviolet noise for the underlying coherent structure to be revealed.

As a guide to identifying this structure, we note the fact that  $\langle q(x)q(0) \rangle \leq 0$ ,  $|x| > 0$ , in the continuum [13]. This implies that the topological charge cannot be predominantly concentrated in 4-dimensional sign-coherent structures of finite physical size [10]. However, one cannot conclude that the local behavior of topological charge density is strictly disordered! Indeed, the negativity of the correlator does not exclude enhanced sign-coherence present on *lower-dimensional* subsets of 4-d space-time. In that case the structure could respect the negativity of the correlator by appropriate embedding of subsets with alternating sign into space-time. Consequently, we focus our search on the level of sign-coherence, and how it changes when concentrating on space-time subregions containing strong fields. In what follows we will refer to sign-coherence in  $q_x$  simply as coherence.

For the numerical study we use  $q_x$  associated with the overlap Dirac operator [6], whose suitability for this pur-

pose was confirmed in Ref. [14]. To sample the QCD vacuum, we work with Wilson gauge backgrounds as summarized in Table I. Configurations are separated by 20,000 sweeps and the Sommer parameter serves to set the scale using the interpolation formula of Ref. [15]. Since the computation is extremely time-consuming, the ensembles are small. However, the attempts to understand QCD vacuum structure in the path integral framework implicitly rely on the expectation that relevant individual configurations exhibit common qualitative properties that are “typical” of the QCD vacuum, so that interesting results should be obtainable from even a few configurations. In our case, we found that for the aspects discussed below, the behavior is remarkably stable from configuration to configuration (both qualitatively and quantitatively). In fact, one could infer the main results presented here by studying just a single configuration from each ensemble. We are thus confident that our conclusions are not affected by low statistics. Some preliminary results related to this work were presented in Ref. [16]. Details of the fermion implementation can be found in Ref. [2].

1. We start by verifying that  $q_x$  is indeed not dominated by coherent 4-d structures, as argued above. Regardless of their shapes, the possible candidates for such structures must be built of elementary lattice 4-d cubes [17] that are themselves coherent (their sites have the same sign of  $q_x$ ). In fact, we can define the coherent regions on the lattice by finding all coherent 4-d cubes  $\mathcal{C}_x$  (labeled by origin  $x$ ) and identifying maximal *connected* regions built from such cubes. We will say that lattice region  $\mathcal{R} = \{\mathcal{C}_{x_i}; i = 1, \dots, N\}$  is connected, if for arbitrary  $\mathcal{C}_{x_i}, \mathcal{C}_{x_j} \in \mathcal{R}$  there is a sequence  $\mathcal{C}_{y_k}, k = 1, \dots, n$ , such that (a)  $\mathcal{C}_{y_k} \in \mathcal{R}$ , (b)  $y_1 = x_i$ ,  $y_n = x_j$ , and (c)  $\mathcal{C}_{y_k}$  and  $\mathcal{C}_{y_{k+1}}$  share a common face (3-d cube).

We have determined all such regions (“structures”)  $\mathcal{R}_k$  present in a given configuration, and ordered them by the number of lattice sites in the structure,  $N_k$ . If there are 4-d structures of finite physical size dominating in the continuum limit, then at least the largest of these coherent regions should exhibit scaling behavior when the lattice spacing is changed. Since the ensembles  $\mathcal{E}_1, \mathcal{E}_2$  have the same physical volumes, the ratios  $N_k/V$  ( $V$  is the number of lattice points) for typical largest structures should not depend on the lattice spacing. In Fig. 1 (top) we show these ratios for a configuration from both ensembles. Rather than being similar, the ratios drop dramatically at the smaller lattice spacing. To see this on average, we compute the mean value of the ratio including the 5 largest structures per configuration. Fig. 1 reveals that the ratio not only drops, but it drops by a factor larger than the ratio of lattice volumes. This is confirmed by the fact that the average number of 4-d cubes per large structure is about 35.3 at  $a = 0.110$ , and is about 29.4 at  $a = 0.082$ . The volume of structures thus decreases even in lattice units. These considerations not only confirm that 4-d structures do not dominate topological charge fluctuations, but also suggest that such structures might not occur in the continuum at all. In-

ensemble	$\beta$	$a$ [fm]	$V$	$V_p$ [fm <sup>4</sup> ]	configs
$\mathcal{E}_1$	5.91	0.110	12 <sup>4</sup>	3.0	8
$\mathcal{E}_2$	6.07	0.082	16 <sup>4</sup>	3.0	2

TABLE I: Ensembles of Wilson gauge configurations. The global topological charges are (3,0,-2,0,2,-1,-1,3) for  $\mathcal{E}_1$  and (2,1) for  $\mathcal{E}_2$ .

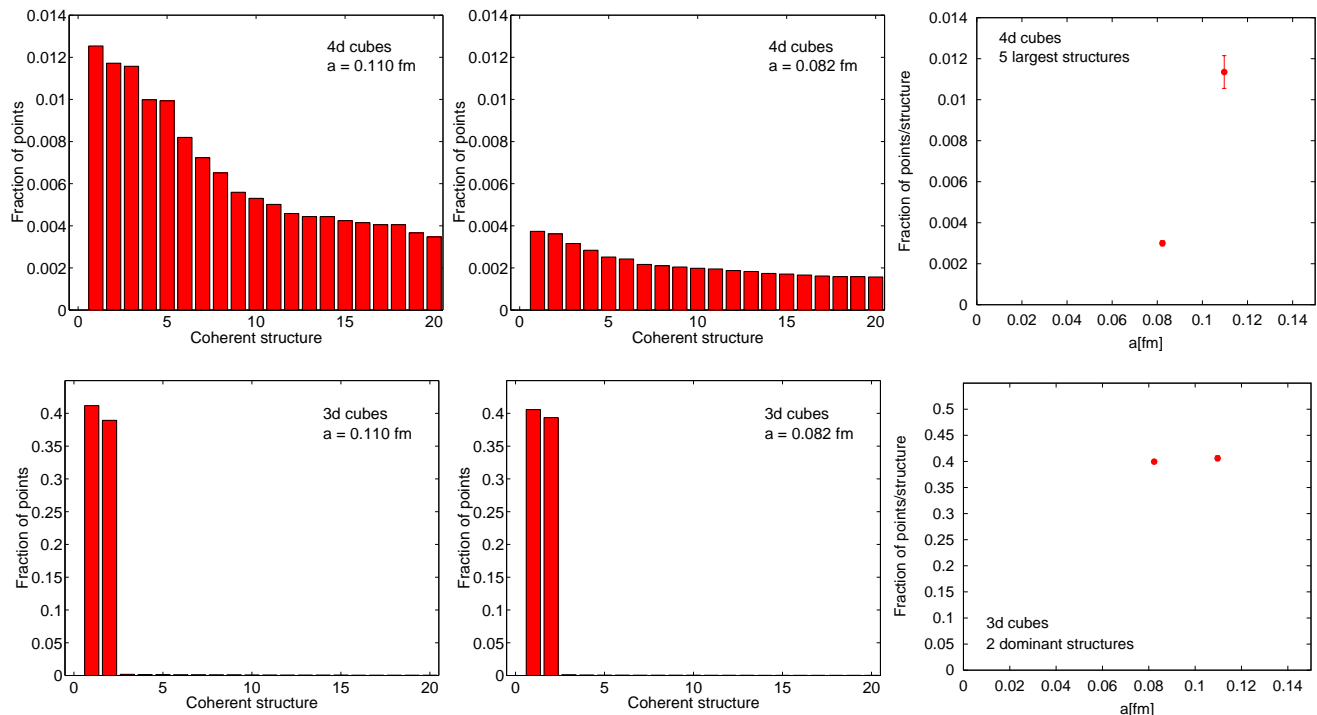


FIG. 1: Top: The fraction of space-time points occupied by the largest 20 structures built of 4-d cubes on a typical configuration from ensemble  $\mathcal{E}_1$  (left) and  $\mathcal{E}_2$  (middle). The average fraction from the 5 largest structures is also shown (right). Bottom: The same as top but for structures built of 3-d cubes. There are error bars on the rhs plots.

deed, in physical units, structures  $\mathcal{R}_k$  observed on the lattice appear to shrink to mere points in the continuum limit.

**2.** We now concentrate on the possibility that  $q_x$  exhibits coherence on lower-dimensional subsets of 4-d space-time. As a first step, we search for maximal coherent regions built from elementary 3-d cubes connected through 2-d faces. Such regions define connected 3-d lattice hypersurfaces embedded in the 4-d space-time. We find that all of the configurations studied (see Table I) exhibit a remarkably similar coherent behavior. The typical situation for a configuration from ensembles  $\mathcal{E}_1$ ,  $\mathcal{E}_2$  is shown in Fig. 1 (bottom). Contrary to the case of 4-d cubes, there are only two (oppositely charged) coherent regions dominating the behavior of  $q_x$ . Together, these folded lattice “sheets” cover about 80% of sites and practically fill the space-time. This situation is insensitive to the change of the lattice spacing and our data indicate that it will survive the continuum limit (bottom right of Fig. 1).

We wish to emphasize two points. First, we have tested whether the existence of the 2-sheet structure reflects a specific order present in  $q_x$ , or if it could occur in a random situation as well. To do that, we have performed a random permutation of sites  $p(x)$  on our lattices and looked for the coherent behavior in  $q_{p(x)}$ . The typical result of such a test is shown in Fig. 2. The 2-sheet structure disappears and the fractions involved are almost invisible on the scale of the original plot. Secondly, the existence of (almost) space-filling 3-d *lattice* sheets is not

sufficient to conclude that the local dimension of maximal coherent regions in the continuum limit is three. The determination of this dimension requires a scaling analysis which is in preparation. While possibly less than three, the dimension is at least one (see part 4 below). Note that this issue is not addressed by the lower right-hand plot of Fig. 1. There the implied scaling relates to the fact that the sheets occupy a macroscopic fraction of space-time and hence involve an infinitely large lower-dimensional manifold in the continuum limit (in the 4-d volume of finite physical size).

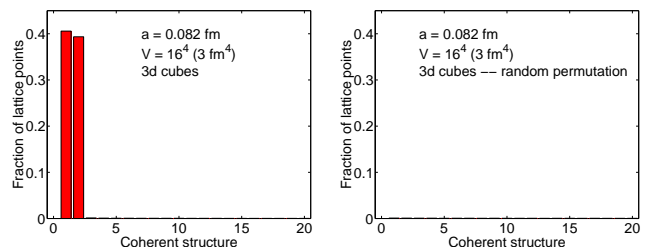


FIG. 2: A typical coherent structure before and after the random permutation of sites. On the common scale, the fractions on the r.h.s. plot are barely visible. Configuration from  $\mathcal{E}_2$ .

**3.** Since the 2-sheet structure almost fills the space-time, it is expected that for a generic point  $x$  on a given sheet, there are points  $y$  on the same sheet separated from  $x$  by maximal space-time distances possible. Because the sheet is path-connected, such points can be connected by

paths within the sheet. Thus, from the geometric point of view there is no specific long-distance scale (other than infrared cutoff) associated with global behavior of the sheet. We will refer to such a situation occurring in the coherent structure as the *super-long-distance* property [18].

The super-long-distance property might be relevant to the physics of the QCD vacuum, e.g. to Goldstone boson propagation, if it remains true also if one concentrates on regions with largest topological charge density. Indeed, the physics of the vacuum is expected to be mostly driven by fluctuations with intense fields. For a given configuration, let  $\mathcal{S}^f$  ( $0 < f \leq 1$ ) be the subset of the lattice containing the  $fV$  most intense sites  $x$ , as ranked by  $|q_x|$ . Within  $\mathcal{S}^f$ , there are maximal coherent regions  $\mathcal{R}_k^{d,f} \subset \mathcal{S}^f$ ,  $k = 1, 2, \dots, N^{d,f}$ , built from  $d$ -dimensional cubes connected through  $(d-1)$ -dimensional faces. For  $x \in \mathcal{S}^f$  one can find a maximal Euclidean distance  $r_{d,x}^f$  reachable from  $x$  by traveling on a path within a single structure  $\mathcal{R}_k^{d,f} \ni x$ . Note that  $r_{d,x}^f = 0$  for points that do not belong to any structure. Considering a fixed small fraction  $f_0 < f$ , we calculate the average of  $r_{d,x}^f$  over  $x \in \mathcal{S}^{f_0}$ , i.e.  $r_d^{f_0,f} \equiv \langle r_{d,x}^f \rangle_{\mathcal{S}^{f_0}}$ . This provides us with the measure (scale) of how extended the coherent structure typically is. In Fig. 3 we show the  $f$ -dependence of  $r_d^{0.01,f}$  measured in units of the largest Euclidean distance  $(\sum_{i=1}^4 L_i^2)^{1/2}/2$  ( $L_i$  are the sizes of the lattice box). The average is taken over the ensemble  $\mathcal{E}_1$  and the observed behavior is typical (and stable) for  $f_0$  of a few percent. Also shown is the result after performing the random permutation of sites for every configuration.

Note that in the case of 4-d cubes the structure never becomes super-long-distance. In fact, we expect that the maximal distance will approach zero in the continuum limit at arbitrary  $f$ . For  $d = 3, 2, 1$ , we observe

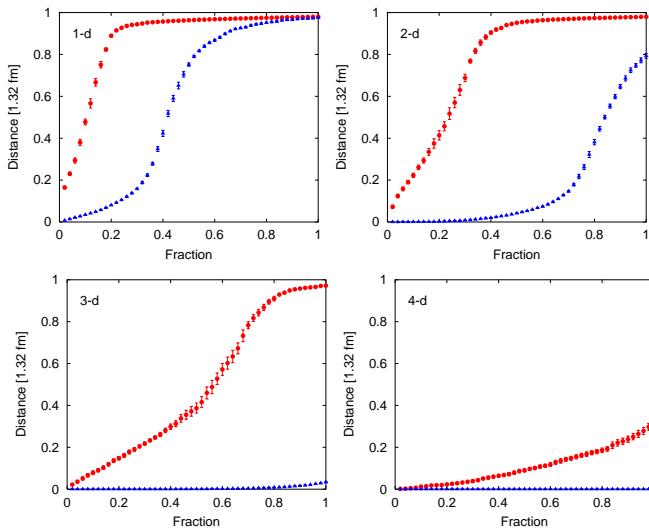


FIG. 3: The  $f$ -dependence of  $r_d^{0.01,f}$  for ensemble  $\mathcal{E}_1$  (upper curves of each plot) and after random permutation of sites (lower curves of each plot). Results using 1,2,3 and 4-dimensional hypercubes are shown.

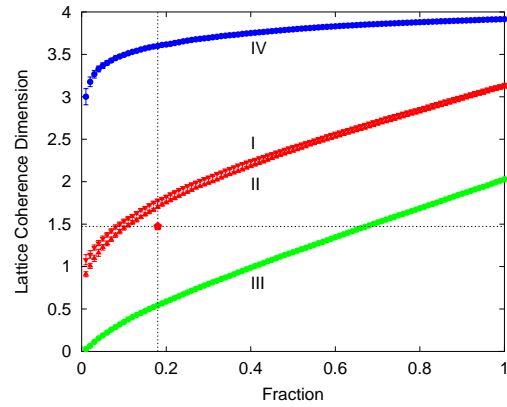


FIG. 4: Lattice coherence dimension. Explanation in text.

a well-defined transition to a super-long-distance state which is certainly present at  $f \approx 0.8, 0.4, 0.2$  respectively ( $r_d^{0.01,f} \approx 0.9$  at those fractions). These values are insensitive to the change of the lattice spacing. We thus see that after removing the low-intensity points, the super-long-distance structure remains at the core if lower-dimensional elementary cubes are used. The minimal structure with this property is exposed with 1-d cubes (links) and we will refer to it as the *skeleton*. In our numerical experiments, the maximal space-time distances start occurring already at about  $f = 0.16$  while the average saturates at about  $f = 0.20$ . We thus take  $f = 0.18$  as our initial reference value for the skeleton. As further evidence that the observed structure carries a significant amount of order, we note that at  $f = 0.18$  (with the skeleton already formed) one is still confined to average maximal distances of a single lattice spacing when random permutation of sites is performed.

4. Even without an extensive scaling analysis, it is possible to obtain useful insight into the question of the actual space-time dimension involved in the skeleton. More precisely, we will discuss the *local* dimension. To appreciate the difference, consider e.g. a network built from 1-d lines, but organized globally into a 2-d structure (“mesh”) with a typical physical distance  $l$  among the nodes. Locally, such a manifold is 1-dimensional, but on the scales larger than  $l$  it will appear 2-dimensional. We will consider the global structure from this point of view elsewhere.

Our tool here will be the *lattice local dimension*  $d^L(\mathcal{S})$  which we define for an arbitrary subset  $\mathcal{S}$  of the lattice. For  $x \in \mathcal{S}$  let  $d_x^L$  be the maximal dimension  $d$  of the elementary cube  $\mathcal{C}_y^d$  such that  $x \in \mathcal{C}_y^d$  and  $\mathcal{C}_y^d \subset \mathcal{S}$ , i.e. the maximal dimension of the cube within  $\mathcal{S}$  containing  $x$ . Then  $d^L(\mathcal{S}) \equiv \langle d_x^L \rangle_{\mathcal{S}}$  is the average of this local dimension over  $\mathcal{S}$ . While  $d^L(\mathcal{S})$  is strictly a lattice notion, it can still be quite useful. In particular, if there is an underlying set  $\mathcal{S}^c$  in the continuum characterized by a single local dimension  $d(\mathcal{S}^c) < 4$ , then the continuum limit of  $d^L(\mathcal{S})$  typically provides an upper bound for  $d(\mathcal{S}^c)$ . For example, consider a line of non-zero physical length in the continuum. At sufficiently small lattice spacing this

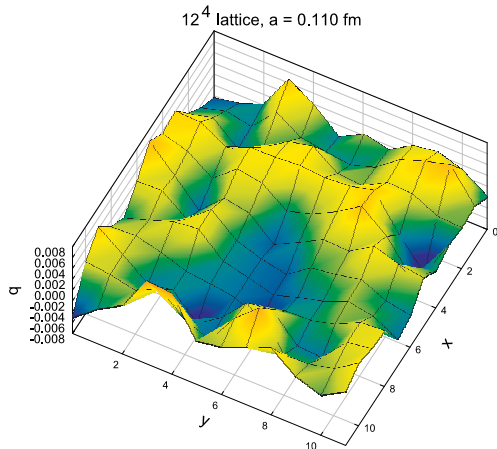


FIG. 5: Generic behavior of  $q_x$  on a 2-d section of space-time (configuration from  $\mathcal{E}_1$ ).

might appear as the connected structure built predominantly of bonds, in which case the continuum limit of  $d^L(\mathcal{S})$  coincides with  $d(\mathcal{S}^c)$ . However, it might also come as a string of mainly 4-d cubes at arbitrarily small lattice spacing, and then the limit of  $d^L(\mathcal{S})$  will be significantly larger than  $d(\mathcal{S}^c)$ . At the same time,  $d^L(\mathcal{S}) \geq 1$  for the *connected* lattice structures and the physical dimension will not be underestimated.

Since the super-long-distance property involves connected parts spreading over maximal distances, and since it is insensitive to the change of lattice spacing, we can conclude that the skeleton is at least 1-dimensional. To see whether higher dimensions (less than four) could be relevant we consider sets  $\mathcal{S}^f$  and their partitions  $\mathcal{S}^f = \mathcal{S}^{f+} \cup \mathcal{S}^{f-}$  into coherent subsets containing sites with positive and negative sign of  $q_x$ . In Fig. 4 we show the  $f$ -dependence of the average *lattice coherence dimension*  $\langle d^L(\mathcal{S}^{f\pm}) \rangle$  for ensembles  $\mathcal{E}_1$  (I) and  $\mathcal{E}_2$  (II). We see that the dimension slightly *decreases* as we approach the continuum limit. The naive linear extrapolation for the skeleton value  $f = 0.18$  (pentagon) gives  $\langle d^L(\mathcal{S}^{f\pm}) \rangle \approx 1.5$  in the continuum limit and we thus conclude that the physical local dimension associated with the skeleton is  $1 \leq d \lesssim 1.5$ . Assuming that the local structure is not fractal (an option to be investigated) we are thus led to the conclusion that the skeleton is locally 1-dimensional.

For comparison, we show in Fig. 4 also  $\langle d^L(\mathcal{S}^{f\pm}) \rangle$  for  $\mathcal{E}_2$  after random permutation of sites (III), and the result for effective density  $q_x^{(\Lambda=750 \text{ MeV})}$  at the same lattice spacing (IV). As expected, the curve (III) lies lower and tends to zero smoothly at small fractions. On the other hand, for the effective density one naively expects 4-d coherence on the scale  $1/\Lambda$  in the continuum limit, and thus the lattice coherence dimension is much higher.

**5.** Finally, to start developing a visual intuition for the kind of structure we are observing, we now proceed to graphically verify the existence of the coherent sheets described in part 2. To do that, we have studied the graphs of  $q_x$  on 2-d sections of the underlying space-time

torus. The *generic* behavior of  $q_x$  is shown in Fig. 5 (configuration from ensemble  $\mathcal{E}_1$ ). One can clearly observe the enhancement of the structure with linear “ridges” spreading over the whole system. It is easy to see that this is precisely the behavior expected from the (almost) space-filling super-long-distance sheets. Indeed, recall that if  $\Omega$  is an arbitrary base manifold and  $\Omega_1, \Omega_2 \subset \Omega$ , then  $\dim(\Omega_1 \cap \Omega_2) = \dim(\Omega_1) + \dim(\Omega_2) - \dim(\Omega)$  generically. If we identify  $\Omega$  with the 4-d space-time torus,  $\Omega_1$  with the 2-d torus of the section plane, and  $\Omega_2$  with the manifold of the structure, we get

$$\dim(\Omega_1 \cap \Omega_2) = \dim(\Omega_2) - 2 \quad (2)$$

Thus if  $\Omega_2$  is a 3-d super-long-distance hypersurface, we should generically see very extended 1-d regions of sign-coherence, which is precisely what is observed. Thus, at the lattice cutoff of about 2 GeV the sheets behave as 3-d hypersurfaces. The precise local dimension of maximal coherent regions in the continuum limit will be studied elsewhere.

In this work we have addressed the following question. Can we identify a fundamental (incorporating all scales) ordered structure in topological charge density for typical configurations contributing to the pure-gluon QCD path integral? In other words, using nothing more than a *local* operator  $q_x$  to calculate space-time distribution of topological charge, can one detect well-defined patterns in these distributions? While such structure has not been observed before, we have argued that the special properties of the newly available topological charge densities associated with Ginsparg-Wilson fermions give reasons to re-examine this question in detail. In particular, the suppression of ultraviolet noise by *chiral smoothing* suggests that the problem of ultraviolet dominance might be solved and the underlying order could be revealed. Performing numerical experiments, we have then provided evidence for a fundamental structure of this type by showing that topological charge exhibits long-range order (sign-coherence) on lower-dimensional subsets of the 4-d Euclidean space. In this initial study we have concentrated on certain geometrical properties of this structure. Indeed, if topological charge fluctuations play a role in important aspects of the QCD vacuum (such as  $S\chi SB$ ), then some geometrical features should reflect that. While it is not clear yet which structural aspects are physically most relevant, we emphasize two that we find most intriguing: (i) Space-time regions with intense topological charge density are organized into a maximally extended (super-long-distance) structure (“*skeleton*”). This suggests that there is no specific long-distance scale associated with *individual* geometrical objects. Rather, there is a global low-dimensional structure that might have to be considered as a whole. (Distance scales associated with  $\Lambda_{QCD}$  could be reflected by local features of such global structure.) We speculate that the super-long-distance character of the skeleton might be naturally associated with the long-range propagation of Goldstone pions. It will be demonstrated elsewhere that the super-



long-distance property is inherited and *enhanced* at low energy. (ii) Our data indicates that the skeleton is a locally-linear folded structure, much like a protein or a neural network in 3-d. One aspect that might be significant about this result is that the propagation of mass-

less quarks on a 1-d manifold naturally leads to a non-zero density of Dirac eigenvalues around zero, and hence  $S\chi$ SB (see e.g. Ref. [19] for discussion of similar issues). The possibility that such a scenario might be relevant for QCD is being studied.

- 
- [1] I. Horváth, N. Isgur, J. McCune, H.B. Thacker, Phys. Rev. **D65**, 014502 (2002); T. deGrand, A. Hasenfratz, Phys. Rev. **D64**, 034512 (2001).
  - [2] I. Horváth, S.J. Dong, T. Draper, N. Isgur, F.X. Lee, K.F. Liu, J. McCune, H.B. Thacker, J.B. Zhang, Phys. Rev. **D66**, 034501 (2002).
  - [3] T. DeGrand, A. Hasenfratz, Phys. Rev. **D65**, 014503 (2002); I. Hip et al., Phys. Rev. **D65**, 014506 (2002); R. Edwards, U. Heller, Phys. Rev. **D65**, 014505 (2002); T. Blum et al., Phys. Rev. **D65**, 014504 (2002); C. Gattringer et al., Nucl. Phys. **B618** (2001) 205.
  - [4] N. Cundy, M. Teper, U. Wenger, Phys. Rev. **D66**, 094505 (2002); C. Gattringer, Phys. Rev. Lett. **88** 221601 (2002); P. Hasenfratz et al., Nucl. Phys. **B643** (2002) 280; C. Gattringer, Phys. Rev. **D67**, 034507 (2003).
  - [5] H. Neuberger, Nucl. Phys. **B** (Proc. Suppl.) 83-84 (2000) 67; M. Creutz, Rev. Mod. Phys. 73 (2001) 119; F. Niedermayer Nucl. Phys. **B** (Proc. Suppl.) 73 (1999) 105.
  - [6] H. Neuberger, Phys. Lett. **B427** (1998) 353.
  - [7] P. Hasenfratz, V. Laliena, F. Niedermayer, Phys. Lett. **B427** (1998) 125.
  - [8] R. Narayanan, H. Neuberger, Nucl. Phys. **B443**, (1995) 305; M. Lüscher, Nucl. Phys. **B568** (2000) 162.
  - [9] L. Giusti, G.C. Rossi, M. Testa, G. Veneziano, Nucl. Phys. **B628** (2002) 234.
  - [10] I. Horváth, S.J. Dong, T. Draper, F.X. Lee, K.F. Liu, H.B. Thacker, J.B. Zhang, Phys. Rev. **D67**, 011501(R) (2003).
  - [11] E. Witten, Nucl. Phys. **B149**, 285 (1979).
  - [12] I. Horváth, Phys. Rev. Lett. **81** (1998) 4063; I. Horváth, C.T. Balwe, R. Mendris, Nucl. Phys. **B599**, 283 (2001).
  - [13] E. Seiler, I.O. Stamatescu, MPI-PAE/Pth 10/87; E. Seiler, Phys. Lett. **B525**, 355 (2002).
  - [14] I. Horváth, S.J. Dong, T. Draper, F.X. Lee, K.F. Liu, J.B. Zhang, H.B. Thacker, Nucl. Phys. **B** (Proc. Suppl.) 119 (2003) 688.
  - [15] M. Guagnelli, R. Sommer, H. Wittig, Nucl. Phys. **B535** (1998) 389.
  - [16] I. Horváth, S.J. Dong, T. Draper, K.F. Liu, N. Mathur, F.X. Lee, H.B. Thacker, J.B. Zhang, **hep-lat/0212013**.
  - [17] We will refer to elementary “links, squares, cubes and hypercubes” of 4-dimensional lattice uniformly as 1-d cubes, 2-d cubes, etc.
  - [18] It is tempting to refer to such structure also as a “percolating structure”. However, at this stage it is not clear whether similarities to percolation go beyond the unbounded nature of the structure.
  - [19] G. Tiktopoulos, Phys. Rev. **D35**, 732 (1987); J.M. Cornwall, G. Tiktopoulos, Phys. Lett. **B181**, 353 (1986); H. Reinhardt, private communication.